Magnetic phase diagrams of spin systems with inversion asymmetry

S.J. Venema
Bachelor Thesis
Supervisor: R.A. Duine
Institute for Theoretical Physics, Utrecht University

June 17, 2014

Abstract

We construct a phase diagram for bulk magnetic materials and thin film materials that lack inversion symmetry, with the external field and anisotropy as parameters. Three states occur: a homogeneous state, a skyrmion lattice state and a spiral state. The phase diagram shows clear phase transitions between the different states as a function of strength of anisotropy and external field. At finite temperature these phase transitions all occur at lower external field.

Contents

1 Introduction

In a magnetic material the energy is mainly determined by the exchange energy. This exchange coupling is called ferromagnetic if the energy is minimized when all spins are aligned and anti-ferromagnetic if the spins are aligned antiparallel. See for example Ref. [1]. When one applies a sufficiently large external magnetic field the magnetization will align with the external field. Clearly, this will be the state which minimizes the energy. Besides the exchange energy and the energy due to the external field there can be other energy terms in exotic materials. One example is the Dzyaloshinskii-Moriya interaction which wants the system to form spiral structures [2] and, furthermore, there is the anisotropy which gives a preferential direction for the magnetization to align with in the absence of an external field. The smallest energy term which we will encounter in this thesis comes from the dipole-dipole interaction. This term gives rise to a demagnetizing field; a magnetic field which tends to reduce the magnetic moment of the system.

Dzyaloshinskii-Moriya interactions can lead to skyrmion configurations. Skyrmions are topological objects in which the magnetization has a spiral-like configuration [3]. These skyrmions have been observed in bulk materials like MnSi [4, 5] and in thin film materials [6]. In Fig. (1) the experimental phase diagram of MnSi is shown, with on the horizontal axis the temperature and on the vertical axis the magnetic field. We see a conical state, a helical state, a homogeneous state and an A-phase. The conical state and the helical state are both one-dimensional spiral states, whereas the A-phase is the skyrmion state.

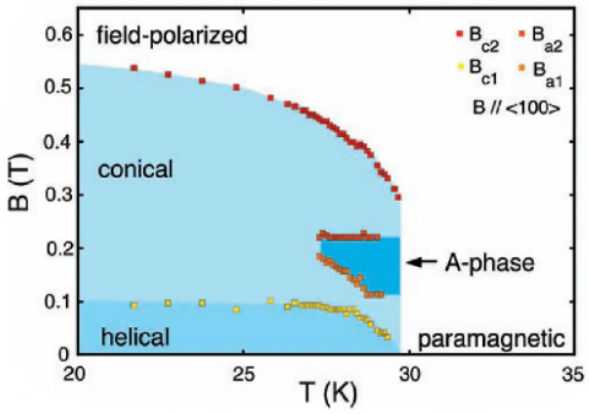

Figure 1: Experimental phase diagram of MnSi [4].

Skyrmions are relatively small and easy to move with a low electrical current density. These properties make them good candidates for usage in spintronic storage or logic devices [7]. The spacing between bits would be of the order of the skyrmion diameter, which is of the order of nanometres. This small size and shorter spacing could lead to faster information flow or smaller current densities, which in the end means a lower energy consumption.

In this Thesis we find phase diagrams for bulk magnetic materials and magnetic thin film materials. First we investigate the systems at zero temperature. This was also done in Ref. [8] and Ref. [9]. We look at a single skyrmion to find the governing equations. Then we generalize this to a lattice of skyrmions. After that, we look at possible spiral states. Spiral states are one-dimensional

configurations where the magnetization is spiraling around a certain axis. We calculate, for different values of the external field, which state minimizes the energy at a given anisotropy. This will give us a phase diagram of the system at zero temperature. The system can be in a homogeneous state, a skyrmion state or in a spiral state. We compare this phase diagram with results from Monte-Carlo simulations [10]. In the second part of this Thesis we add temperature to our discussion by using the Landau free energy. Within certain approximations we will again calculate a phase diagram for T/T_c=0.5 and compare it with results from Monte-Carlo simulations. We end in Chapter (7) with our conclusions.

2 Dzyaloshinskii-Moriya interaction

For clarity we first explicitly state the two forms of Dzyaloshinskii-Moriya interaction we will use. These will be used in the next chapter. These interactions arise from spin-orbit-coupling in combination with lack of inversion symmetry [11]. In bulk materials like MnSi the energy term is often [8]

$$E_{DM} = \int \mathrm{d}\mathbf{x} \frac{C}{2} \mathbf{\Omega} \cdot (\nabla \times \mathbf{\Omega}), \tag{1}$$

where C is the Dzyaloshinskii-Moriya interaction constant and $\mathbf{\Omega}(\mathbf{x})$ the unit magnetization vector. We will use this energy term for the bulk material case. This term causes vortex-like skyrmions as shown in Fig. (2a). In thin films the energy term for the Dzyaloshinskii-Moriya interaction is [8]

$$E_{DM} = \int \mathrm{d}\mathbf{x} \frac{C}{2} \left(\hat{y} \cdot \left(\mathbf{\Omega} \times \frac{\partial \mathbf{\Omega}}{\partial x} \right) - \hat{x} \cdot \left(\mathbf{\Omega} \times \frac{\partial \mathbf{\Omega}}{\partial y} \right) \right). \tag{2}$$

We will use this term for thin film materials. This term favors hedgehog-like skyrmions as shown in Fig (2b)

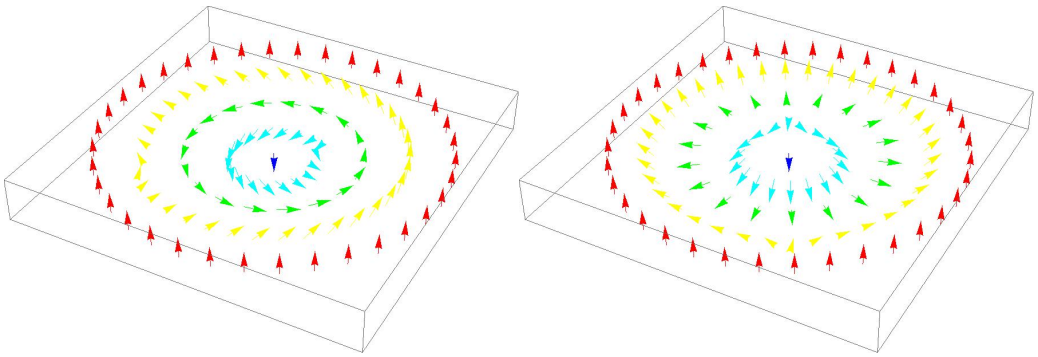

(a) vortex skyrmion (b) hedgehog skyrmion

Figure 2: Two different skyrmion configurations.

3 Single skyrmion at zero temperature

In this chapter we investigate a single skyrmion at zero temperature. We try to find the governing equations for the skyrmion which we then generalize to skyrmions in a lattice.

3.1 Bulk material

We follow the discussion of Ref. [12] to find the unit magnetization vector $\mathbf{\Omega}(\mathbf{x})$. The energy of the magnetic configuration in a bulk material is given by

$$E[\mathbf{\Omega}(\mathbf{x})] = \int \mathrm{d}\mathbf{x}\Big\{ -\frac{J_s}{2}\mathbf{\Omega}\cdot\nabla^2\mathbf{\Omega} + \frac{C}{2}\mathbf{\Omega}\cdot(\nabla\times\mathbf{\Omega}) + K(1-\Omega_z^2) + \mu_0 HM(1-\Omega_z) - \mu_0 M\mathbf{\Omega}\cdot\mathbf{H_d}\Big\}, \tag{3}$$

where J_s is the spin stiffness, C the Dzyaloshinskii-Moriya interaction constant, K the anisotropy constant and μ_0 the vacuum permeability. The external magnetic field H is applied in the $\hat{z}$-direction and is taken positive. $\mathbf{H_d}$ is the demagnetizing (or stray) field and M is the saturation magnetization. The saturation magnetization is the length of the magnetization vector $\mathbf{M}$, so with the unit magnetization vector we get $\mathbf{M}(\mathbf{x}) = M\mathbf{\Omega}(\mathbf{x})$. We now write $\mathbf{\Omega}(\mathbf{x})$ as

$$\mathbf{\Omega}(\mathbf{x}) = \sin\theta\cos\phi_0\,\hat{\rho} + \sin\theta\sin\phi_0\,\hat{\varphi} + \cos\theta\,\hat{z}, \tag{4}$$

where θ can depend in principle on all cylindrical coordinates $\mathbf{x} = (\rho, \varphi, z)$. The angle ϕ_0 is a constant which determines whether the skyrmion is a hedgehog-like or a vortex-like skyrmion. Furthermore we are assuming that we have rotational symmetry in the $\hat{\varphi}$-direction and translational symmetry in the $\hat{z}$-direction. This means that the θ now only depends on ρ. Using the parametrization from Eq. (4), we find the energy

$$\epsilon[\theta(\rho)] \equiv \frac{E[\theta(\rho)]}{2\pi L_z} = \int \mathrm{d}\rho\Big\{ \frac{J_s}{2}\left(\left(\frac{\mathrm{d}\theta}{\mathrm{d}\rho}\right)^2 + \frac{\sin^2\theta}{\rho^2}\right) + \frac{C}{2}\sin\phi_0\left(\frac{\mathrm{d}\theta}{\mathrm{d}\rho} + \frac{\sin\theta\cos\theta}{\rho}\right) + K\sin^2\theta + \mu_0 HM(1-\cos\theta) - \mu_0 M\mathbf{\Omega}\cdot\mathbf{H_d}\Big\}\rho, \tag{5}$$

where the integration over φ and z gives $2\pi L_z$. We divide the energy by this quantity to get the energy density per unit length in the z-direction. Now we only need to find an expression for the demagnetizing field $\mathbf{H_d}$. This field must satisfy Maxwell's equations:

$$\nabla\times\mathbf{H_d} = 0; \tag{6a}$$

$$\nabla\cdot\mathbf{H_d} = -M(\nabla\cdot\mathbf{\Omega}). \tag{6b}$$

Because the curl of the stray field is zero there exists a scalar potential U such that $\mathbf{H_d} = \nabla U$. Furthermore in the second Maxwell equation $\mathbf{\Omega}$ only depends on ρ so $\mathbf{H_d}$ and thus U also depends only on ρ. Filling in the scalar potential into the second Maxwell equation and using Eq. (4) we get

$$M(\nabla\cdot\mathbf{\Omega}) = M\cos\phi_0\left(\cos\theta\frac{\mathrm{d}\theta}{\mathrm{d}\rho} + \frac{\sin\theta}{\rho}\right) = -\nabla\cdot\mathbf{H_d} = -\nabla^2 U = -\frac{\mathrm{d}^2U}{\mathrm{d}\rho^2} - \frac{1}{\rho}\frac{\mathrm{d}U}{\mathrm{d}\rho}. \tag{7}$$

This means that $\frac{1}{\rho}\frac{\mathrm{d}U}{\mathrm{d}\rho} = -M\cos\phi_0\frac{\sin\theta}{\rho}$, so the stray field which satisfies the Maxwell equations becomes

$$\mathbf{H_d} = -M\cos\phi_0\sin\theta\hat{\rho}. \tag{8}$$

Putting this in the energy density gives

$$\begin{aligned}\epsilon[\theta(\rho)] = \int d\rho\Bigg\{\frac{J_s}{2}\left(\left(\frac{\mathrm{d}\theta}{\mathrm{d}\rho}\right)^2 + \frac{\sin^2\theta}{\rho^2}\right) + \frac{C}{2}\sin\phi_0\left(\frac{\mathrm{d}\theta}{\mathrm{d}\rho} + \frac{\sin\theta\cos\theta}{\rho}\right) + K\sin^2\theta \\ + \mu_0 HM(1-\cos\theta) + \mu_0 M\cos^2\phi_0\sin^2\theta\Bigg\}\rho.\end{aligned} \tag{9}$$

In a bulk material the energy density is minimized when $\phi_0 = \pi/2$ [12]. The energy density then becomes

$$\begin{aligned}\epsilon[\theta(\rho)] = \int \mathrm{d}\rho\Bigg\{\frac{J_s}{2}\left(\left(\frac{\mathrm{d}\theta}{\mathrm{d}\rho}\right)^2 + \frac{\sin^2\theta}{\rho^2}\right) + \frac{C}{2}\left(\frac{\mathrm{d}\theta}{\mathrm{d}\rho} + \frac{\sin\theta\cos\theta}{\rho}\right) + K\sin^2\theta \\ + \mu_0 HM(1-\cos\theta)\Bigg\}\rho.\end{aligned} \tag{10}$$

The corresponding Euler equation is

$$J_s\left(\frac{\mathrm{d}^2\theta}{\mathrm{d}\rho^2} + \frac{1}{\rho}\frac{\mathrm{d}\theta}{\mathrm{d}\rho} - \frac{\sin\theta\cos\theta}{\rho^2}\right) + C\frac{\sin^2\theta}{\rho} - 2K\sin\theta\cos\theta - \mu_0 HM\sin\theta = 0, \tag{11}$$

We introduce $\tilde{\rho} = \frac{C}{J_s}\rho$ to get a dimensionless position variable and divide Eq. (11) by C^2/J_s. In this way we get a dimensionless Euler equation

$$\frac{\mathrm{d}^2\theta}{\mathrm{d}\tilde{\rho}^2} + \frac{1}{\tilde{\rho}}\frac{\mathrm{d}\theta}{\mathrm{d}\tilde{\rho}} - \frac{\sin\theta\cos\theta}{\tilde{\rho}^2} + \frac{\sin^2\theta}{\tilde{\rho}} - \beta\sin\theta\cos\theta - \frac{h}{2}\sin\theta = 0, \tag{12}$$

with dimensionless constants $\beta = \frac{2J_sK}{C^2}$ and $h = \frac{2\mu_0 J_s HM}{C^2}$. We cannot solve this equation analytically so we solve it numerically. We take the magnetization to be in the negative $\hat{z}$-direction at $\tilde{\rho} = 0$ and in the positive $\hat{z}$-direction at $\tilde{\rho} = \infty$, so the boundary conditions are $\theta(0) = \pi$ and $\theta(\tilde{\rho}\to\infty) = 0$. See also Fig. (2) In Fig. (3) the solutions $\theta(\tilde{\rho})$ are shown for various values of β and h.

3.2 Thin films

In the previous part we considered a skyrmion in a bulk material with translational and rotational invariance. We now look at a thin layer of cobalt between two layers of platinum [12]. This system is two dimensional. We use the same parametrization as in the bulk material without the z-component, so $\mathbf{x} = (\rho, \varphi)$. The energy of the thin film is

$$\begin{aligned}E[\mathbf{\Omega}(\mathbf{x})] = t_c\int \mathrm{d}\mathbf{x}\Bigg\{-\frac{J_s}{2}\mathbf{\Omega}\cdot\nabla^2\mathbf{\Omega} + \frac{C}{2}\left(\hat{y}\cdot\left(\mathbf{\Omega}\times\frac{\partial\mathbf{\Omega}}{\partial x}\right) - \hat{x}\cdot\left(\mathbf{\Omega}\times\frac{\partial\mathbf{\Omega}}{\partial y}\right)\right) \\ + K(1-\Omega_z^2) + \mu_0 HM(1-\Omega_z) - \mu_0 M\mathbf{\Omega}\cdot\mathbf{H_d}\Bigg\},\end{aligned} \tag{13}$$

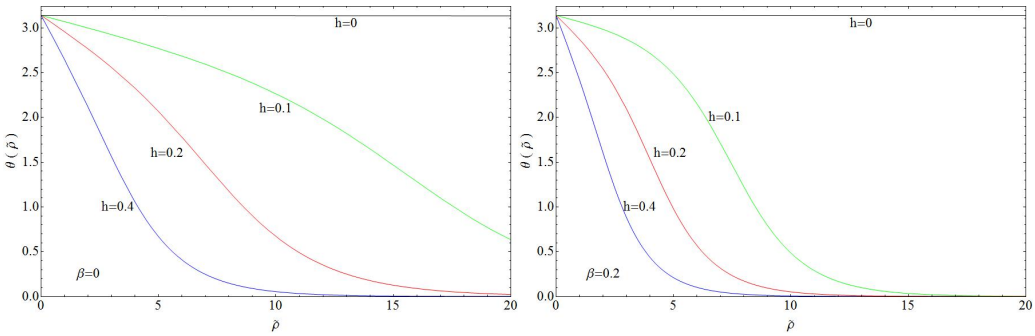

(a) β=0 (b) β=0.2

Figure 3: $\theta(\tilde{\rho})$ for different values of β and h for the single skyrmion.

with t_c the thickness of the cobalt layer. We see that only the Dzyaloshinskii-Moriya interaction is different from the bulk material. We fill in the parametrization for $\mathbf{\Omega}$ given in Eq. (4). this yields

$$\epsilon[\theta(\rho)] \equiv \frac{E[\theta(\rho)]}{2\pi t_c} = \int d\rho \Bigg\{ \frac{J_s}{2}\left(\left(\frac{\mathrm{d}\theta}{\mathrm{d}\rho}\right)^2 + \frac{\sin^2\theta}{\rho^2}\right) + \frac{C}{2}\cos\phi_0\left(\frac{\mathrm{d}\theta}{\mathrm{d}\rho} + \frac{\sin\theta\cos\theta}{\rho}\right) + K\sin^2\theta + \mu_0 HM(1-\cos\theta) + \mu_0 M^2\cos^2\phi_0\sin^2\theta \Bigg\}\rho. \tag{14}$$

Minimizing this energy and rewriting the result in a dimensionless form gives

$$\frac{\mathrm{d}^2\theta}{\mathrm{d}\tilde{\rho}^2} + \frac{1}{\tilde{\rho}}\frac{\mathrm{d}\theta}{\mathrm{d}\tilde{\rho}} - \frac{\sin\theta\cos\theta}{\tilde{\rho}^2} + \cos\phi_0\frac{\sin^2\theta}{\tilde{\rho}} - (\beta + \lambda\cos^2\phi_0)\sin\theta\cos\theta - \frac{h}{2}\sin\theta = 0, \tag{15}$$

where $\lambda = \frac{2\mu_0 M^2 J_s}{C^2}$. Typical values for h, β and λ are h= 0.72, β=16 and λ=9.0 [13]. With these values the skyrmion will be in the hedgehog configuration, so ϕ_0=0 [12]. We now have a differential equation which has the same form as Eq. (15), the Euler equation for the bulk material. We only have to replace β with $\beta + \lambda$.

4 Phase diagram

There are several states possible in the magnetic materials of interest to us here. The system can be in a homogeneous state where all spins are pointing in one direction. If the skyrmions have a finite radius there can exist a lattice of skyrmions and there can be spiral states in the system. To find out which state is established for different values of the external magnetic field h we have to find out which state has the lowest energy. We then calculate where the phase transitions take place and summarize this in a phase diagram.

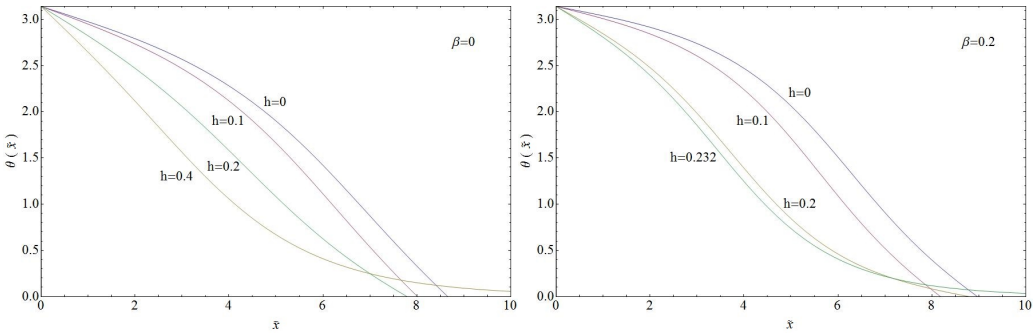

(a) β=0 (b) β=0.2

Figure 4: $\theta(\tilde{x})$ for a skyrmion with a finite radius for different values of β and h.

4.1 Skyrmions in a lattice

First we look at the skyrmion state. In the previous section we have found the skyrmion configuration of a single skyrmion in a bulk material and in a thin film. Now we investigate a lattice of skyrmions. We follow the discussion of Ref. [8]. We take the skyrmion lattice to be triangular so that the unit cell containing one skyrmion has a hexogonal form. This hexagonal form is difficult to treat mathematically so we use circles to approximate the hexagonal form. In this way the skyrmions are rotationally symmetric as in the single skyrmion situation. The boundary conditions will be as follows. In the middle of the skyrmion we have boundary condition $\theta(0) = \pi$ and on the outer circle we have $\theta(R) = 0$. The mean energy density per unit volume for a thin film is

$$w[\theta(\rho)] = \frac{2}{R^2}\int_0^R \mathrm{d}\rho\Bigg\{\frac{J_s}{2}\left(\left(\frac{\mathrm{d}\theta}{\mathrm{d}\rho}\right)^2 + \frac{\sin^2\theta}{\rho^2}\right) + \frac{C}{2}\left(\frac{\mathrm{d}\theta}{\mathrm{d}\rho} + \frac{\sin\theta\cos\theta}{\rho}\right) + K\sin^2\theta + \mu_0 HM(1 - \cos\theta) + \mu_0 M\sin^2\theta\Bigg\}\rho\mathrm{d}\rho. \tag{16}$$

The last term drops out in a bulk material. We now have the energy density divided by the area of the skyrmion, so where we had an energy density in the single skyrmion case we now have a mean energy density. The Euler equation is the same as that of the single skyrmion and is given in Eq. (15), except now the boundary conditions are different. We cannot solve this equation analytically, but we can make a linear approximation to get an estimate of the energy density. We take $\theta(\tilde{\rho}) = \pi(1 - \tilde{\rho}/R)$ so that it satisfies the boundary conditions. Filling in this function into Eq. (16) we get the following function for the mean dimensionless energy density

$$\tilde{w}(R) = \frac{12.3073}{R^2} - \frac{\pi}{R} + 0.5\beta + 0.5947h. \tag{17}$$

Minimizing this mean energy density with respect to R we find $R = 7.835$. If h=0 and β=0 we find with this radius a dimensionless mean energy density of $\tilde{w} = -0.20$.

We now turn to solving this problem numerically. To find the radius of the skyrmions in the lattice we calculate the mean energy density for various values for the radius. The radius corresponding to the lowest mean energy density will be the radius of the skyrmion in the lattice

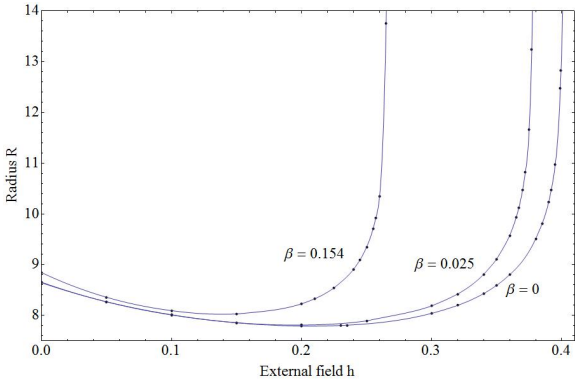

Figure 5: The radius of the skyrmion against the external magnetic field for some values of β in a bulk material, so $\lambda = 0$.

under the circular cell approximation. In Fig. (5) this minimum mean energy density radius is plotted for different values of h and β. We see that if h=0 and β=0 the radius is of the same order as our linear approximation. Now we know the radius we can use the boundary conditions to solve the Euler equation. $\theta(\tilde{\rho})$ is shown in Fig. (4) for different values of β and h.

4.2 Spiral State

Now we look at spiral states. These spiral states are one dimensional configurations. For the spiral state we also consider the bulk material and the thin film.

4.2.1 Spiral state in a thin film

First we consider spirals in a thin film. Since the spiral states are one dimensional we can choose them to vary only along the x-axis. Assuming $\mathbf{\Omega}$ only lies in the $x - z$ plane we get the following parametrization of the unit magnetization vector

$$\mathbf{\Omega}(x) \;=\; -\sin\theta(x)\hat{x} \;+\; \cos\theta(x)\hat{z}. \tag{18}$$

This gives a spiral in the $x - z$ plane as shown in Fig. (6) [9]. With this magnetization the mean

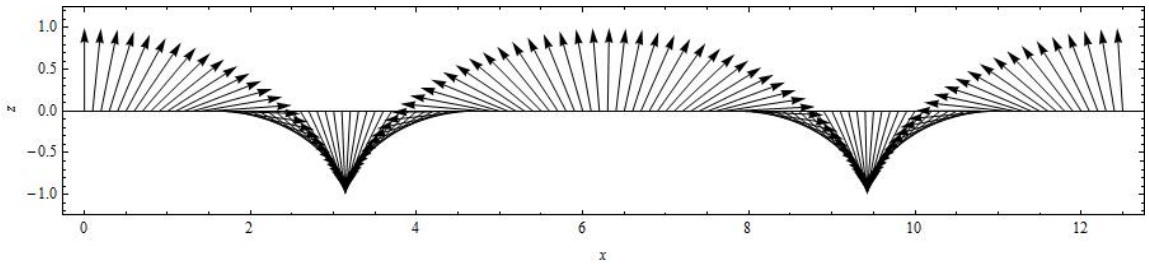

Figure 6: A spiral state along the $\hat{x}$-direction in the $x - z$ plane.

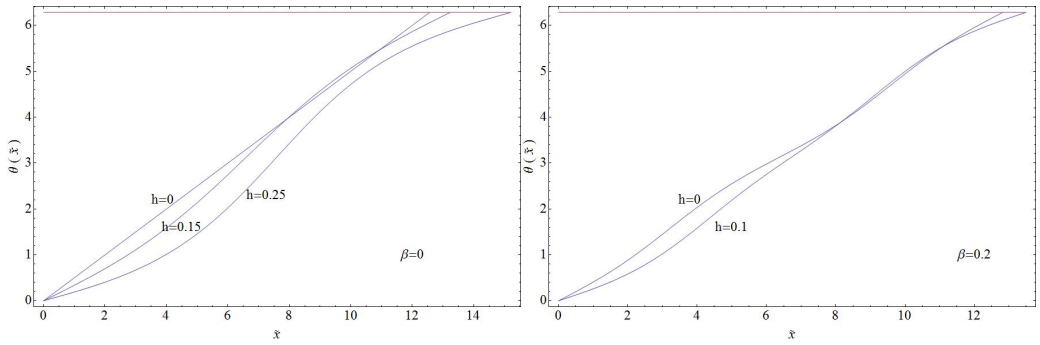

(a) β=0 (b) β=0.2

Figure 7: $\theta(\tilde{x})$ for different values of β and h for the spiral state.

dimensionless energy density for the spiral state becomes

$$\epsilon[\theta(x)] = \frac{1}{\tilde{x}_0}\int_0^{\tilde{x}_0} \mathrm{d}x\left\{\left(\frac{\partial\theta}{\partial\tilde{x}}\right)^2 - \left(\frac{\partial\theta}{\partial\tilde{x}}\right) + \beta\sin^2\theta + h(1-\cos\theta) - \frac{\lambda}{M}\mathbf{\Omega}\cdot\mathbf{H_d}\right\}, \tag{19}$$

with $\beta = \frac{2KJ_s}{C^2}$, $h = \frac{2\mu_0 HMJ_s}{C^2}$ and $\lambda = \frac{2\mu_0 M^2 J_s}{C^2}$, the same variables as in the skyrmion case. Furthermore, $\tilde{x}_0$ is the period of the spiral. The stray field $\mathbf{H_d}$ needs to satisfy the Maxwell equations given in Eq. (6). Following the same procedure as with the skyrmion demagnetizing field we find the stray field

$$\mathbf{H_d} = -M\Omega_x(x)\hat{x}. \tag{20}$$

So the associated energy density becomes

$$\epsilon_{stray} = \int \mathrm{d}x\,\lambda\sin^2\theta. \tag{21}$$

Using this the Euler equation for the spiral state becomes

$$\frac{\mathrm{d}^2\theta}{\mathrm{d}\tilde{x}^2} = \frac{h}{2}\sin\theta + (\beta+\lambda)\sin\theta\cos\theta. \tag{22}$$

By definition of the spiral, we have the periodic boundary condition

$$\theta(\tilde{x}_0) = \theta(0) + 2\pi. \tag{23}$$

We can solve the case when h=0 and $\beta+\lambda$=0 analytically. The Euler equation then becomes

$$\frac{\mathrm{d}^2\theta}{\mathrm{d}\tilde{x}^2} = 0. \tag{24}$$

Solutions are of the form $\theta(\tilde{x}) = a\tilde{x} + b$. With the periodic boundary condition we see that $a = 2\pi/\tilde{x}_0$ and b will be a phase factor in which we can take zero. So $\theta(x) = 2\pi/\tilde{x}_0 x$ is a linear function which means that the magnetization is a sinusoidal function. Inserting this into Eq. (19)

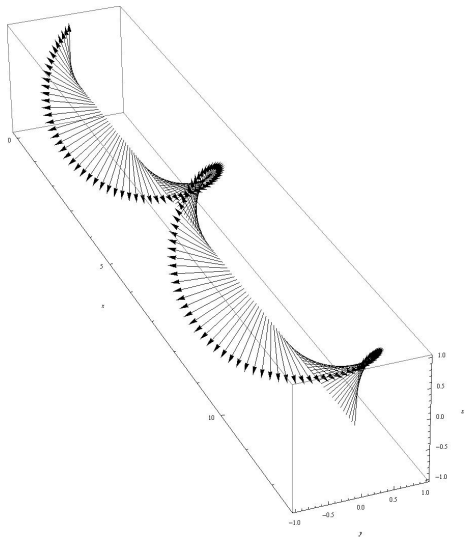

Figure 8: A spiral along the x-axis with the magnetization lying in the $y-z$ plane.

and minimizing with respect to $\tilde{x}_0$ we get a period of $\tilde{x}_0 = 4\pi$. With this period the dimensionless energy density is $\epsilon = -1/4$. To find solutions for other values of h and β we numerically solve the Euler equation. Solving Eq. (19) for different values of the period $\tilde{x}_0$ gives a different the mean energy density for each period. The period with the lowest value of the energy density will be the actual period of the spiral state. Now that we know the period we can use the periodic boundary condition to solve the Euler equation. In Fig. (7) $\theta(\tilde{x})$ is shown for different values of h and β.

4.2.2 Spiral state in a bulk material

We now consider a spiral state in a bulk material. For simplicity we will assume that the spiral will be invariant under translation in the $\hat{z}$-direction. Just like the spiral in the thin film we choose the spiral state to vary along the x-axis. To get a nonzero Dzyaloshinskii-Moriya interaction we choose a parametrization

$$\mathbf{\Omega}(x) \;=\; -\sin\theta(x)\hat{y} \;+\; \cos\theta(x)\hat{z}. \tag{25}$$

This parametrization corresponds to a helical spiral as shown in Fig. (8). The dimensionless energy density then becomes

$$\epsilon[\theta(x)] = \frac{1}{\tilde{x}_0}\int_0^{\tilde{x}_0} \mathrm{d}x \Bigg\{ \left(\frac{\partial\theta}{\partial\tilde{x}}\right)^2 - \left(\frac{\partial\theta}{\partial\tilde{x}}\right) + \beta\sin^2\theta + h(1-\cos\theta) \;-\; \frac{\lambda}{M}\mathbf{H_d}\cdot\mathbf{\Omega}\Bigg\}. \tag{26}$$

We again try to find a stray field which satisfies the Maxwell equations. Following the same procedure as in the skyrmion case we find that the stray field is constant in the $\hat{x}$-direction. This means that it does not contribute to the energy since the magnetization is always perpendicular to the $\hat{x}$-direction.

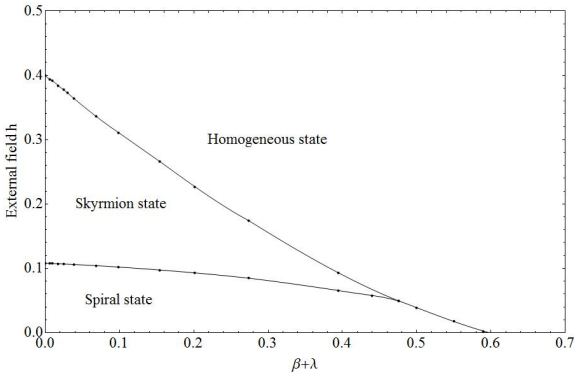

Figure 9: Phase diagram for magnetic systems with inversion asymmetry. λ=0 represents a bulk material, while $\lambda \neq 0$ gives the phase diagram of a thin film material.

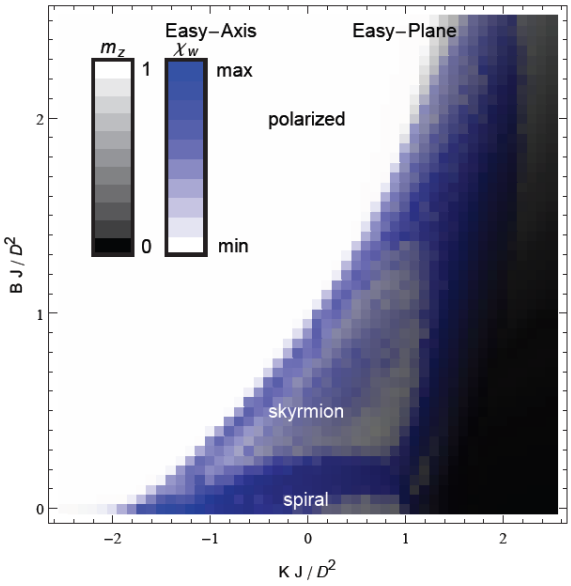

Figure 10: Phase diagram from Monte-Carlo simulations taken from Ref. [10]. Here is $K_{MC}J/D^2$=$-4(K_{Theory}+\mu_0 M^2)J/C^2$=$-2(\beta+\lambda)$ and BJ/D^2= $4\mu_0 HMJ_s/C^2$=$2h$.

4.3 Results

We saw that the mean energy density was $\epsilon_{skyrmion} = -0.20$ for the skyrmion in the linear approximation leading to Eq. (17) and $\epsilon_{spiral} = -1/4$ for the spiral state when $h = 0$ and $\beta + \lambda = 0$. This means that in this case the system will be in a spiral state because it is the state with the lowest energy. We now determine the phase transitions by calculating for different values of $\beta + \lambda$ the external field h for which the energy density of both states is the same. We get the phase diagram given in Fig. (9). If we take $\beta + \lambda = 0$ we see that there is a homogeneous state for external field

greater than $h = 0.400$, we get a skyrmion state for h between $h = 0.400$ and $h = 0.108$, and a spiral state for external fields lower than $h = 0.108$. Furthermore we see that there is a triple point at $\beta + \lambda = 0.4766$ where the external field is $h = 0.0490$.

We compare this theoretical result with results from Monte-Carlo Simulations [10]. In this Thesis we only look at the easy- axis configuration. We see in Fig. (10) that the general form of the phase diagram from the Monte-Carlo simulations is in agreement with our theoretical result. Furthermore we see that for $\beta + \lambda$=0 the phase transition from skyrmion state to homogeneous state occurs between $h = 0.4$ and $h = 0.5$ in the Monte-Carlo simulations where our theory predicts $h = 0.400$. We find the phase transition from spiral state to skyrmion state between $h = 0.05$ and $h = 0.15$ in the Monte-Carlo simulations. This is also similar to our theoretical found value of $h = 0.108$. We find the triple point between $\beta + \lambda = 0.4$ and $\beta + \lambda = 0.6$ at an external field of $h = 0.05$ in the Monte-Carlo simulations which is also in agreement with our theory.

5 Finite temperature phase diagram

Until now we have only looked at the zero temperature case. Now we will include temperature into our discussion of the phase diagram. To do this we will look at the Landau free energy instead of the energy. The Landau free energy for bulk materials is given by

$$\begin{aligned} F[\mathbf{\Omega}(\mathbf{x})] = \int \mathrm{d}\mathbf{x} \Big\{ &- \frac{J_s'}{2}\mathbf{m}\cdot\nabla^2\mathbf{m} + \frac{C'}{2}\mathbf{m}\cdot(\nabla\times\mathbf{m}) + K'(1-m_z^2) \\ &+ \mu_0 H(1-m_z) - \mu_0\mathbf{m}\cdot\mathbf{H_d} + \alpha(T)\mathbf{m}^2 + \gamma_0\mathbf{m}^4 \Big\}, \end{aligned} \tag{27}$$

with $\mathbf{m}$ the magnetization vector, J_s' the spin stiffness at finite temperature, C' the Dzyaloshinskii-Moriya interaction constant at finite temperature and K' the anisotropy constant at finite temperature. We write this vector in terms of a length and a direction , so $\mathbf{m}(\mathbf{x}) = m(\mathbf{x})\,\mathbf{\Omega}(\mathbf{x})$.

5.1 Skyrmion in a bulk material

We first consider the skyrmion state. Filling in the parametrization for $\mathbf{\Omega}$ given in Eq. (4) gives

$$\begin{aligned} f[\theta(\rho), m(\rho)] = \int \mathrm{d}\rho \Big\{ &\frac{J_s'}{2}\left(m^2\left(\frac{\mathrm{d}\theta}{\mathrm{d}\rho}\right)^2 + \frac{m^2\sin^2\theta}{\rho^2} - m\frac{\mathrm{d}^2 m}{\mathrm{d}\rho^2}\right) + \frac{C'}{2}m^2\sin\phi_0\left(\frac{\mathrm{d}\theta}{\mathrm{d}\rho} + \frac{\sin\theta\cos\theta}{\rho}\right) \\ &+ K'm^2\sin^2\theta + \mu_0 H m(1-\cos\theta) - \mu_0 m\cos^2\phi_0\sin^2\theta + \alpha(T)m^2 + \gamma_0 m^4 \Big\}\rho. \end{aligned} \tag{28}$$

Here we have assumed translational invariance in the $\hat{z}$-direction and rotational invariance in the $\hat{\varphi}$-direction. α depends on the temperature and γ_0 is a constant. We assume there will be a vortex like skyrmion just as in the zero temperature case, so $\phi_0 = \pi/2$. Now we can minimize this equation with respect to θ and with respect to m. Then we get two coupled Euler equations. Minimizing with respect to m gives

$$\begin{aligned} J_s'\left(\frac{m\sin^2\theta}{\rho} + m\rho\left(\frac{\mathrm{d}\theta}{\mathrm{d}\rho}\right)^2 - \frac{\mathrm{d}m}{\mathrm{d}\rho} - \rho\frac{\mathrm{d}^2 m}{\mathrm{d}\rho^2}\right) + C'\rho m\left(\frac{\mathrm{d}\theta}{\mathrm{d}\rho} + \frac{\sin\theta\cos\theta}{\rho}\right) \\ + 2mK'\rho\sin^2\theta + \mu_0 H\rho(1-\cos\theta) + 2\alpha(T)\rho m + 4\gamma_0\rho m^3 = 0. \end{aligned} \tag{29}$$

Minimizing with respect to θ gives

$$J_s'\left(m^2\rho\frac{\mathrm{d}^2\theta}{\mathrm{d}\rho^2} + m^2\frac{\mathrm{d}\theta}{\mathrm{d}\rho} - \frac{m^2\sin\theta\cos\theta}{\rho} + 2m\rho\frac{\mathrm{d}m}{\mathrm{d}\rho}\frac{\mathrm{d}\theta}{\mathrm{d}\rho}\right) + C'\left(\rho m\frac{\mathrm{d}m}{\mathrm{d}\rho} + m^2\sin^2\theta\right) - 2m^2K'\rho\sin\theta\cos\theta - \mu_0 Hm\rho\sin\theta = 0. \tag{30}$$

For simplicity we assume that Eq. (29) can be approximated by

$$2\alpha(T)m + 4\gamma m^3 = 0. \tag{31}$$

We can solve this equation analytically and assuming that $\alpha(T) = \alpha_0(T - T_c)$, with α_0 a constant and T_c the critical temperature we get

$$m_0(T) = \pm\sqrt{\frac{\alpha_0(T_c - T)}{2\gamma_0}}. \tag{32}$$

So the length m only depends on the temperature but not on the position. We can now simplify Eq. (30) to

$$J_s'\left(m_0^2\frac{\mathrm{d}^2\theta}{\mathrm{d}\rho^2} + m_0^2\frac{1}{\rho}\frac{\mathrm{d}\theta}{\mathrm{d}\rho} - \frac{m_0^2\sin\theta\cos\theta}{\rho^2}\right) + C'\frac{m_0^2\sin^2\theta}{\rho} - 2m_0^2K'\sin\theta\cos\theta - \mu_0 Hm_0\sin\theta = 0. \tag{33}$$

From this equation we can derive what J_s', C' and K' are. Filling in T=0 should give back Eq. (11). So this gives $J_s'm_0^2(0) = J_s$, $C'm_0(0)^2 = C$, $K'm_0(0)^2 = K$ and $m_0(0) = M$. With this the remaining Euler equation becomes

$$\left(\frac{\mathrm{d}^2\theta}{\mathrm{d}\rho^2} + \frac{1}{\rho}\frac{\mathrm{d}\theta}{\mathrm{d}\rho} - \frac{\sin\theta\cos\theta}{\rho^2}\right) + \frac{\sin^2\theta}{\rho} - \beta\sin\theta\cos\theta - \frac{h}{2\sqrt{1-\tilde{T}}}\sin\theta = 0, \tag{34}$$

Where we have defined the dimensionless variables $\tilde{T} = T/T_c$ and $\tilde{m}(\tilde{T}) = m_0(\tilde{T})/m_0(0)$. This equation is essentially the same as the one at zero temperature. Only where we first had h we now have $h/\sqrt{1-\tilde{T}}$. This means that to get the equation at finite temperature h needs to be lower in order to get the same number in the equation.

5.2 Spiral in a bulk material

Next we will consider the spiral state. We again use $\mathbf{m} = m\mathbf{\Omega}$ but now we use the parametrization of Eq.(18). We again assume that the spiral varies along the x-axis. We get the energy density

$$f[\theta(x), m(x)] = \frac{1}{\tilde{x}_0}\int_0^{\tilde{x}_0}\mathrm{d}x\{-\frac{J_s'}{2}\left(m\frac{\mathrm{d}^2m}{\mathrm{dx}^2} - m^2\left(\frac{\mathrm{d}\theta}{\mathrm{dx}}\right)^2\right) - \frac{C'}{2}m^2\frac{\mathrm{d}\theta}{\mathrm{dx}} + K'm^2\sin^2\theta + \mu_0 Hm(1-\cos\theta) + \alpha(T)m^2 + \gamma_0 m^4\}. \tag{35}$$

minimizing this with respect to m we get

$$\begin{aligned} -J_s' \left(\frac{1}{2} \frac{\mathrm{d}^2 m}{\mathrm{dx}^2} \, - \, m \left(\frac{\mathrm{d}\theta}{\mathrm{dx}} \right)^2 \right) \, - \, C' m \frac{\mathrm{d}\theta}{\mathrm{dx}} \, + \, 2K' m \sin^2 \theta \\ + \mu_0 H (1 - \cos\theta) \, + 2\alpha(T) m + 4\gamma_0 m^3 \, = \, 0 \end{aligned} \tag{36}$$

and with respect to θ

$$\begin{aligned} J_s' \left(2m \frac{\mathrm{d}m}{\mathrm{dx}} \frac{\mathrm{d}\theta}{\mathrm{dx}} \, + \, m^2 \frac{\mathrm{d}^2 \theta}{\mathrm{dx}^2} \right) \, - \, C' m \frac{\mathrm{d}m}{\mathrm{dx}} \\ -2K' m^2 \sin\theta \cos\theta \, - \, \mu_0 H m \sin\theta \, = \, 0. \end{aligned} \tag{37}$$

Again assuming Eq. (31) as an approximation for Euler equation (36) gives Eq. (32) for the length and filling this into the other Euler equation gives

$$J_s' \, m_0^2 \frac{\mathrm{d}^2 \theta}{\mathrm{dx}^2} \, - \, 2K' m_0^2 \sin\theta \cos\theta \, - \, \mu_0 H m_0 \sin\theta \, = \, 0. \tag{38}$$

Rewriting J_s', C' and K' into J_s, C and K with the relations found earlier and then making this equation dimensionless gives

$$\frac{\mathrm{d}^2 \theta}{\mathrm{d}\tilde{\mathrm{x}}^2} \, - \, \beta \sin\theta \cos\theta \, - \, \frac{h}{2\sqrt{1 - \tilde{T}}} \sin\theta \, = \, 0. \tag{39}$$

We see that the external field h in the equation for zero temperature also has to be replaced by $h/(2\sqrt{1-\tilde{T}})$ to get the same equation. This means that the phase transitions occur at an lower external field if the temperature increases. This can be understood from the fact that the external field competes with the other energies, mostly the Dzyaloshinskii-Moriya interaction and the anisotropy. The finite temperature makes these effectively smaller.

5.3 Finite temperature in a thin film

The Landau free energy for a thin film is

$$\begin{aligned} F[\mathbf{\Omega}(\mathbf{x})] \, = t_c \int \mathrm{d}\mathbf{x} \Big\{ \, - \, \frac{J_s'}{2} \mathbf{m} \cdot \nabla^2 \, \mathbf{m} \, + \, \frac{C'}{2} \left(\hat{y} \cdot \left(\mathbf{m} \, \times \, \frac{\partial \mathbf{m}}{\partial x} \right) \, - \, \hat{x} \cdot \left(\mathbf{m} \, \times \, \frac{\partial \mathbf{m}}{\partial y} \right) \right) \\ + \, K'(1 \, - \, m_z^2) \, + \, \mu_0 H (1 \, - \, m_z) \, - \, \mu_0 \mathbf{m} \cdot \mathbf{H_d} \, + \, \alpha(T) \mathbf{m}^2 \, + \, \gamma_0 \mathbf{m}^4 \Big\}, \end{aligned} \tag{40}$$

where t_c is the width of the film. Working this out analogous to the bulk material we find that the only difference with the bulk material is an extra the stray field term. We find the stray field which satisfies the Maxwell equations in the same way as in the previous sections. It turns out that the stray field is

$$\mathbf{H_d} \, = \, -m \sin\theta \hat{\rho}, \tag{41}$$

for the skyrmion in the thin film and

$$\mathbf{H_d} \, = \, m \, \sin\theta \hat{x}, \tag{42}$$

for the spiral state in the thin film. Minimizing the Landau free energy for the skyrmion and the spiral state gives the same equations as in the bulk material, but both with an extra term. The equations become

$$\left(\frac{\mathrm{d}^2\theta}{\mathrm{d}\tilde{\rho}^2} + \frac{1}{\tilde{\rho}}\frac{\mathrm{d}\theta}{\mathrm{d}\tilde{\rho}} - \frac{\sin\theta\cos\theta}{\tilde{\rho}^2}\right) + \frac{\sin^2\theta}{\tilde{\rho}} - (\beta+\lambda)\sin\theta\cos\theta - \frac{h}{2\sqrt{1-\tilde{T}}}\sin\theta = 0, \tag{43}$$

for the skyrmion state and

$$\frac{\mathrm{d}^2\theta}{\mathrm{d}\tilde{\mathrm{x}}^2} - (\beta+\lambda)\sin\theta\cos\theta - \frac{h}{2\sqrt{1-\tilde{T}}}\sin\theta = 0, \tag{44}$$

for the spiral state.

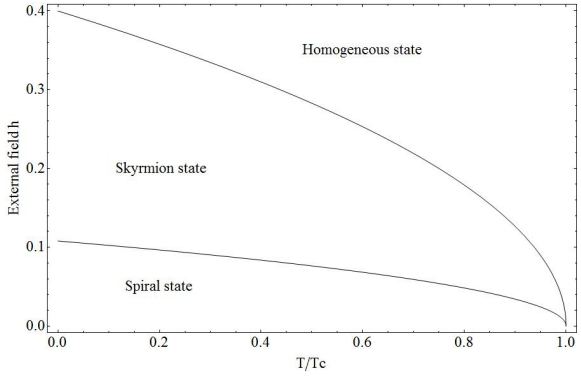

Figure 11: Phase diagram for nonzero temperature for $\beta + \lambda$=0

5.4 Results at finite temperature

In Fig. (11) the phase diagram at finite temperature is shown. Just as in the zero-temperature case we also compare the phase diagram at finite temperature with the corresponding Monte-Carlo simulations [10]. We compare the phase diagram at $\tilde{T}$=0.5. In Fig. (12) the phase diagrams from our theory and the Monte-Carlo simulations are shown. In the theoretical result all phase transitions occur at lower external field h than was the case at zero temperature. This is not generally the case in the Monte-Carlo simulations. The phase transition between the spiral state and the skyrmion state does occur at lower external field in the Monte-Carlo simulations, but the phase transition between the skyrmion state and the homogeneous state does not. This can be explained by thermal fluctuations. The energy of the homogeneous state is calculated for the case when there are no gradiënts so when the magnetization is pointing in one direction in the whole material. At higher temperature this will not be the case. The magnetization will vary slightly from place to place due to thermal fluctuations. This will increase the energy of the homogeneous state and thus make it favorable to be in the skyrmion state at a higher external field than predicted

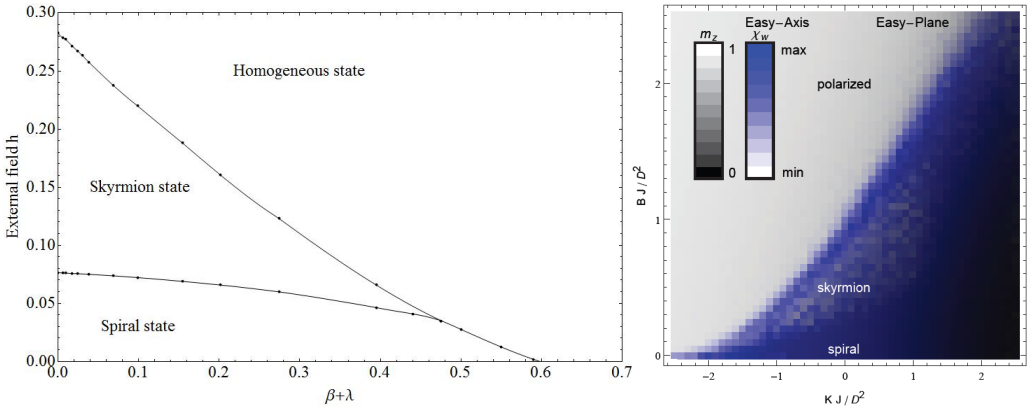

(a) Theoretical phase diagram

(b) Phase diagram from Monte-Carlo simulations.

Figure 12: Phase diagrams at $\tilde{T}$=0.5.

by the theoretical model. We also see that the phase transitions have become less sharp in the Monte-Carlo simulations. This can also be explained by thermal fluctuations. In the region close to the phase transition the energy of both states lies close to each other. This means that due to thermal fluctuations the state with higher energy can temporarily be realized. There will be a region where both states occur which results in a less sharp phase transition in the phase diagram.

6 Improved approximations for finite temperature

In the previous section we approximated Eq. (36) with Eq. (31). The length turned out to be independent of position in this approximation which was given by Eq. (32). We now assume that there will be small fluctuations δm around this value. This is because the spiral still varies along the x-axis we have for the magnetization length $m = m_0(T) + \delta m(x)$. We assume δm is small so that we can neglect quadratic and higher order terms. Furthermore we neglect second order derivatives in δm. The Euler equations for the spiral in a bulk material then become

$$\begin{aligned} -(m_0+\delta m)\left(\frac{\mathrm{d}\theta}{\mathrm{d}\tilde{x}}\right)^2 - (m_0+\delta m)\frac{\mathrm{d}\theta}{\mathrm{d}\tilde{x}} + \beta(m_0+\delta m)\sin^2\theta + \frac{hm_0(0)}{2}(1-\cos\theta) \\ +b(2\alpha(T)(m_0+\delta m) + 4\gamma m_0^3 + 12\gamma m_0^2\delta m) = 0, \end{aligned} \tag{45}$$

with $b = J_s m(0)^2/C^2$ and

$$\begin{aligned} 2(m_0+\delta m)\frac{\mathrm{d}\delta m}{\mathrm{d}\tilde{x}}\frac{\mathrm{d}\theta}{\mathrm{d}\tilde{x}} + (m_0^2+2m_0\delta m)\frac{\mathrm{d}^2\theta}{\mathrm{d}\tilde{x}^2} + (m_0+\delta m)\frac{\mathrm{d}\delta m}{\mathrm{d}\tilde{x}} \\ -\beta(m_0^2+2m_0\delta m)\sin\theta\cos\theta - \frac{hm_0(0)}{2}(m_0+\delta m)\sin\theta = 0. \end{aligned} \tag{46}$$

Dividing by m_0 and neglecting all terms which go like $\delta m/m_0$ gives

$$\begin{aligned} &-\left(\frac{\mathrm{d}\theta}{\mathrm{d}\tilde{\mathrm{x}}}\right)^2 - \frac{\mathrm{d}\theta}{\mathrm{d}\tilde{\mathrm{x}}} + \beta\sin^2\theta + \frac{hm_0(0)}{2m_0}(1-\cos\theta) \\ &+\frac{b}{m_0}(2\alpha(T)(m_0+\delta m) + 4\gamma m_0^3 + 12\gamma m_0^2\delta m) = 0, \end{aligned} \tag{47}$$

and

$$2\frac{\mathrm{d}\delta m}{\mathrm{d}\tilde{\mathrm{x}}}\frac{\mathrm{d}\theta}{\mathrm{d}\tilde{\mathrm{x}}} + (m_0+2\delta m)\frac{\mathrm{d}^2\theta}{\mathrm{d}\tilde{\mathrm{x}}^2} + \frac{\mathrm{d}\delta m}{\mathrm{d}\tilde{\mathrm{x}}} - \beta(m_0+2\delta m)\sin\theta\cos\theta - \frac{hm_0(0)}{2}\sin\theta = 0. \tag{48}$$

We can numerically solve these coupled equations. We use periodic boundary conditions for θ and δm. In Fig. (13) the solution is shown for β=0 and h=0.15. It turns out that the solution for θ only differs slightly from the result found with Eq. (32) and Eq. (37). We also see that δm is a periodic function which is much smaller than m_0 so our assumptions still hold.

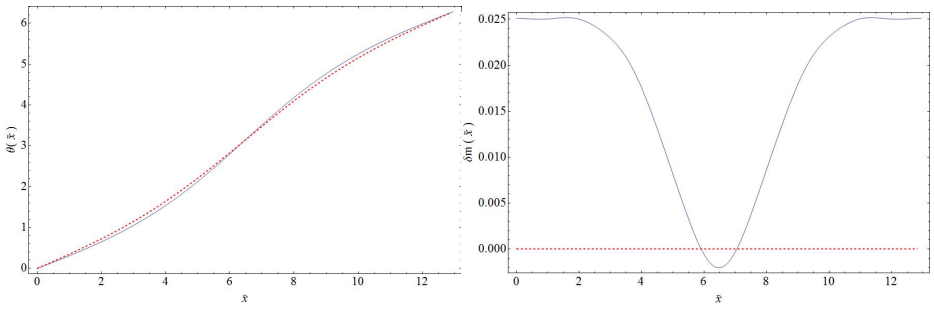

(a) $\theta(\tilde{x})$. (b) $\delta m(\tilde{x})$.

Figure 13: Solution for the linearized Euler equations at $\tilde{T} = 0.5$, h=0.15 and β=0. The blue line is the result found with the improved approximation and the dashed red line is the result from Eq. (32) and Eq. (37).

7 Conclusions

In this Thesis we have determined the phase diagrams in bulk materials and thin films at zero temperature and at finite temperature with an external field and the anisotropy as parameters. Besides a homogeneous state the systems can be in a skyrmion state or a spiral state. The spiral state will occur when the external field and the anisotropy are both small, while the homogeneous state will occur when the external field or the anisotropy are large. In between there will be the skyrmion state. At non-zero temperature the whole external field is multiplied with a factor $\sqrt{1-\tilde{T}}$ so that the phase transitions occur at a lower external field. The solutions found with the improved approximation discussed in Sec. (6) show that our approximation of taking the magnitude of the magnetization constant is reasonable in the case of a spiral. For the skyrmion state however, we only have the constant m_0 approximation. A possible direction for future research is to find an improved approximation for the skyrmion case as well. Furthermore, we only have considered the static case. Further research can be done by studying the dynamics of skyrmions.

References

[1] M.P. Marder, Condensed Matter physics (2010).
[2] I.E. Dzyaloshinsky, Sov. Phys. JETP 5 (1957) 1259.
[3] T.H.R. Skyrme, Nucl. Phys. **31**,556-569 (1962).
[4] S. Mühlbauer et al. Science **323**, 915-919 (2009)
[5] A. Neubauer et al. Phys. Rev. Lett. **102**, 186602 (2009).
[6] S. Heinze et al. Nature Phys. **7**, 713-718 (2011).
[7] A. Fert, V. Cros, J. Sampaio, Nature Nanotechnology **8**, 152-156 (2013).
[8] A. Bogdanov, A. Hubert, J. Magn. Magn. Mater. **138**, 255 (1994).
[9] S. Banerjee, J. Rowland, O Erten, M. Randeria, arXiv:1402.7082v1 (2014).
[10] R. Keesman, Unpublished results (2014).
[11] K. Everschor, Current-induced dynamics of chiral magnetic structures: skyrmions, emergent electrodynamics and spin-transfer torques, PhD Thesis, Universität zu Köln (2012).
[12] M.E. Knoester, Skyrmions driven by the spin Hall effect, Bachelor Thesis, Utrecht University (2013).
[13] S. Emori, U. Bauer, S. Ahn, E. Martinez, G.S.D. Beach, Nature Materials **12**, 611-616 (2013).